

Article

# Regioselective Hydroxylation of Naringin Dihydrochalcone to Produce Neeriocitrin Dihydrochalcone by CYP102A1 (BM3) Mutants

Thi Huong Ha Nguyen <sup>1,†</sup>, Su-Min Woo <sup>1,†</sup>, Ngoc Anh Nguyen <sup>1</sup>, Gun-Su Cha <sup>2</sup>, Soo-Jin Yeom <sup>1,3</sup>, Hyung-Sik Kang <sup>1,3,\*</sup>  and Chul-Ho Yun <sup>1,3,\*</sup> 

<sup>1</sup> School of Biological Sciences and Biotechnology, Graduate School, Chonnam National University, Yongbong-ro 77, Gwangju 61186, Korea; huongha0207@gmail.com (T.H.H.N.); dntnals0@gmail.com (S.-M.W.); ngocanh61093@gmail.com (N.A.N.); soojin258@chonnam.ac.kr (S.-J.Y.)

<sup>2</sup> Namhae Garlic Research Institute, 2465-8 Namhaedaero, Gyeongsangnamdo 52430, Korea; gscha450@gmail.com

<sup>3</sup> School of Biological Sciences and Technology, Chonnam National University, Yongbong-ro 77, Gwangju 61186, Korea

\* Correspondence: kanghs@jnu.ac.kr (H.-S.K.); chyun@jnu.ac.kr (C.-H.Y.); Tel.: +82-62-530-2195 (H.-S.K.); +82-62-530-2194 (C.-H.Y.)

† These authors equally contributed.

Received: 23 June 2020; Accepted: 21 July 2020; Published: 23 July 2020



**Abstract:** Naringin dihydrochalcone (DC) is originally derived from the flavonoid naringin, which occurs naturally in citrus fruits, especially in grapefruit. It is used as an artificial sweetener with a strong antioxidant activity with potential applications in food and pharmaceutical fields. At present, enzymatic and chemical methods to make products of naringin DC by hydroxylation reactions have not been developed. Here, an enzymatic strategy for the efficient synthesis of potentially valuable products from naringin DC, a glycoside of phloretin, was developed using *Bacillus megaterium* CYP102A1 monooxygenase. The major product was identified to be neeriocitrin DC by NMR and LC-MS analyses. Sixty-seven mutants of CYP102A1 were tested for hydroxylation of naringin DC to produce neeriocitrin DC. Six mutants with high activity were selected to determine the kinetic parameters and total turnover numbers (TTNs). The  $k_{cat}$  value of the most active mutant was  $11 \text{ min}^{-1}$  and its TTN was 315. The productivity of neeriocitrin DC production increased up to  $1.1 \text{ mM h}^{-1}$ , which corresponds to  $0.65 \text{ g L}^{-1} \text{ h}^{-1}$ . In this study, we achieved a regioselective hydroxylation of naringin DC to produce neeriocitrin DC.

**Keywords:** CYP102A1; naringin dihydrochalcone; neeriocitrin dihydrochalcone; regioselective hydroxylation

## 1. Introduction

Dihydrochalcone (DC) is a bicyclic flavonoid family with two aromatic rings and a saturated C3 bridge [1]. DC compounds are mainly found in citrus fruits, grapefruits, and apples, and they play an important role in resisting biotic or abiotic stresses in plant [2,3]. To date, more than 200 DC compounds have been identified from over 30 plant families [4]. As DC compounds show strong antioxidant activities, a large number of studies have researched the potential benefits of DC compounds to human health. They were demonstrated to be effective in preventing different physiopathological processes [3], notably diabetes [5] and bone resorption [6]. In recent years, scientists have more often been attracted by in vitro and in vivo biological activities of DC compounds.

Naringin DC (3,5-dihydroxy-4[3-(4-hydroxyphenyl)propanoyl]phenyl 2-O-(6-deoxy- $\alpha$ -L-mannopyranosyl)- $\beta$ -L-glucopyranoside) (Figure 1) is known as a widely used artificial sweetener [7,8]. Naringin DC is produced when naringin is treated with a strong base, such as potassium hydroxide, and then catalytically hydrogenated. Naringin is a flavanone-7-O-glycoside between the flavanone naringenin and the disaccharide neohesperidose. Naringin DC has a sweet value approximately 300 times higher than that of sucrose [9]. Naringin DC has high antioxidant activity, which performs better free-radical scavenging than its corresponding flavanone naringin [10]. Besides, naringin DC is a glycoside of phloretin that shows an inhibitory effect on active transport of glucose into cells by SGLT1 and SGLT2 [8]. Naringin DC was suggested as a promising therapeutic agent for Alzheimer's disease treatment against multiple effects that reduce A $\beta$  levels, suppress neuroinflammation, and enhance neurogenesis [8]. The antioxidant and noncalorie sweetener abilities of naringin DC can make it be a potential compound for applications in food, beverages, and pharmaceuticals [11].

Cytochrome P450 (CYP or P450) is known as one of the largest enzyme families found in all organisms. P450s catalyze the oxidation of various endogenous and xenobiotic compounds [12]. Due to their diversity of substrates, P450s are attractive as biocatalysts for producing chemicals, including bioactive compounds and pharmaceuticals [13,14]. CYP102A1 (P450 BM3) from *Bacillus megaterium* is a self-sufficient monooxygenase enzyme, which is naturally fused to its redox partner, a mammalian-like diflavin reductase. Engineered CYP102A1 mutants have been extensively obtained through rational design and directed evolution to catalyze the oxidation of several non-natural substrates, environmental chemicals, and pharmaceuticals [15–19]. It was also suggested that the engineered CYP102A1 can be developed as a potential biocatalyst for biotechnology applications [20,21].

In this study, we have tried to find an enzymatic strategy for the production of products from naringin DC. A large set of CYP102A1 mutants were used for the efficient synthesis of potentially valuable products from naringin DC. To the best of our knowledge, the enzymatic hydroxylation of naringin DC has not previously been reported. This work is the first report on enzymatic synthesis of neoeriocitrin DC, a major product of naringin DC (Figure 1).

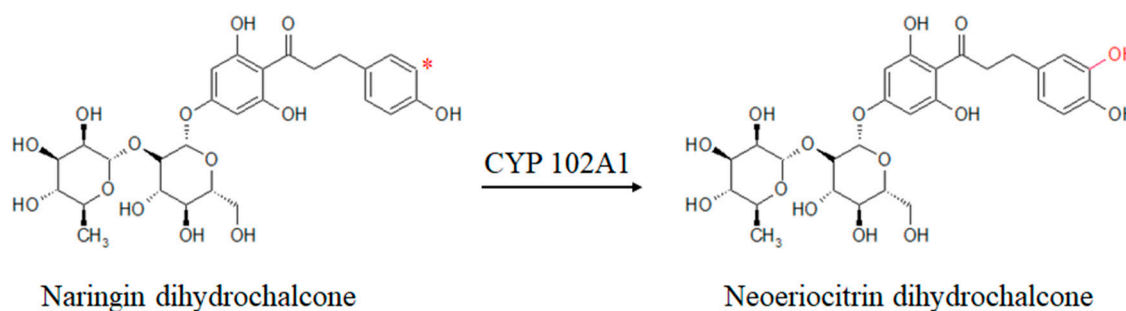


**Figure 1.** Chemical structures of naringin DC and neoeriocitrin DC. The conversion of the substrate, naringin DC, to its corresponding product, neoeriocitrin DC, is catalyzed by CYP102A1 in the presence of NADPH. An enzymatic reaction site on naringin DC is marked by a star.

## 2. Results and Discussion

### 2.1. Hydroxylation of Naringin DC by CYP102A1 Mutants

First, to determine the ability of CYP102A1 to hydroxylate naringin DC, the catalytic activity of the wild type (WT) and its 60 mutants [12,14,19,22–25] toward naringin DC were tested at 200  $\mu$ M substrate for 30 min at 37  $^{\circ}$ C (Figure 2). The 60 mutants used for first screening were selected based on our previous works showing their improved catalytic activities on a number of non-natural substrates, such as natural products and pharmaceuticals (each mutant bears amino acid substitutions relative to WT CYP102A1, as summarized in Supplementary Table S1). To obtain more highly active mutants, the randomized DNA library obtained from the M16V2 library (see Materials and Methods) was screened using a

colorimetric (blue) colony-based method and HPLC analysis (Figure 3). Finally, seven mutants were selected from approximately 500 blue colonies (from M524 to M850 in Supplementary Table S1). The selection was based on the mutants' expression levels and catalytic activity of naringin DC hydroxylation (Figure 2). The mutants M601 ( $7.1 \text{ min}^{-1}$ ), M620 ( $8.2 \text{ min}^{-1}$ ), M788 ( $5.3 \text{ min}^{-1}$ ), and M850 ( $8.0 \text{ min}^{-1}$ ) showed higher catalytic activity than M16V2 ( $3.4 \text{ min}^{-1}$ ).

In the HPLC chromatogram, one minor and one major product were observed (Figure 3). Among all tested mutants, 26 mutants showed apparent but very low activity toward naringin DC ( $<0.5 \text{ min}^{-1}$ ). CYP102A1 WT did not show any apparent activities. Meanwhile, seven mutants (G1, M179, M601, M620, M221, M788, and M850) showed high catalytic activity for naringin DC ( $>5 \text{ min}^{-1}$ ) (Figure 2). Mutants G1 ( $10.2 \text{ min}^{-1}$ ) and M221 ( $9.8 \text{ min}^{-1}$ ) showed approximately three-fold higher catalytic activity toward naringin DC than that of M16V2.

Six mutants were selected for further experiments to determine the kinetic parameters and total turnover numbers (TTNs). M16V2 was selected as it was used as a template to make the DNA library. M179 showed a medium activity and the other four mutants (G1, M221, M620, and M850) had high activities.

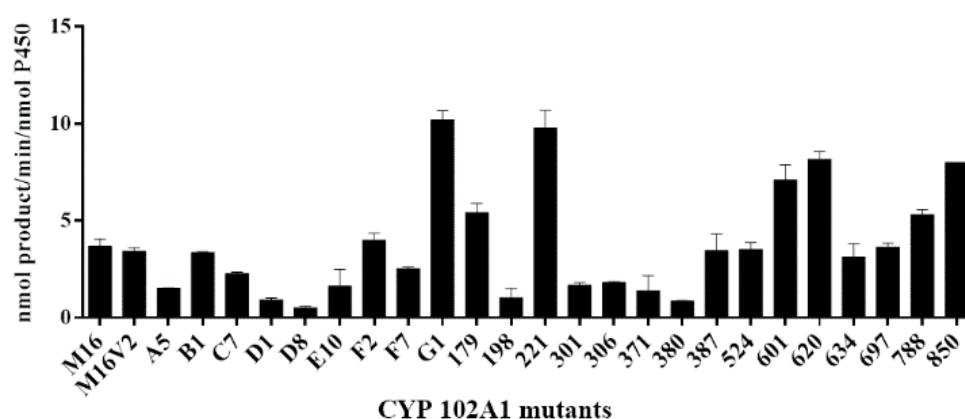


**Figure 2.** Catalytic activity of naringin DC hydroxylation by CYP102A1 mutants. The reactions contained  $200 \mu\text{M}$  naringin DC as a substrate in  $100 \text{ mM}$  potassium phosphate buffer ( $\text{pH } 7.4$ ) and  $0.20 \mu\text{M}$  CYP102A1. NADPH-generating systems were added to initiate the reaction, and the reaction mixtures were incubated for 30 min at  $37 \text{ }^\circ\text{C}$ .

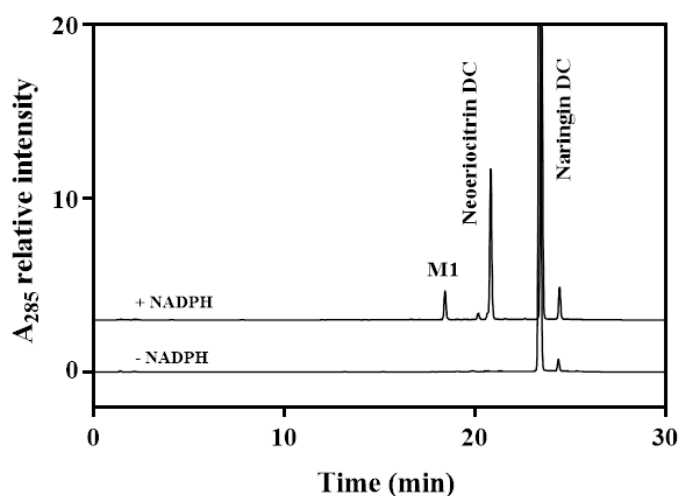


**Figure 3.** HPLC chromatogram of naringin DC and its products formed by CYP102A1 mutant M221. The peaks of reaction mixtures of HPLC chromatograms were identified by comparing their retention times with those of neocitricin DC ( $t_R = 20.8 \text{ min}$ ) and naringin DC ( $t_R = 23.4 \text{ min}$ ). The retention time of M1 was  $18.4 \text{ min}$ .

## 2.2. Optimal Expression of CYP102A1 M221 Mutant

To find the best *Escherichia coli* strain for protein expression of the M221 mutant, the plasmid M221 (in pCW vector) was transformed to a set of competent *E. coli* cells (DH5 $\alpha$ -F'IQ, BL21, SHuffle T7, Rosetta, MG1655, and JM109). The P450 expression levels at different induction periods (12 to 28 h) and incubation temperatures (20 and 25 °C) were analyzed. The MG1655 strain had a higher capability of producing recombinant M221 protein than other strains. Thus, the MG1655 strain was selected for the next experiments. The protein expression level of the M221 enzyme was determined by the evaluation of CO difference spectrum, a typical Fe<sup>2+</sup> CO versus Fe<sup>2+</sup> spectrum of the heme group [26], and obtained after 12 to 28 h culture at 20 and 25 °C. OD<sub>600</sub> and the protein expression level are proportional from 12 to 20 h (Figure 4A). After that, the cell growth rate reached the stationary phase, but the P450 expression level showed difference rates between 20 and 25 °C. At 20 °C, the P450 expression achieved stability up to 28 h. Meanwhile, the P450 expression increased up to 24 h and reached the highest level of approximately 0.5 nmol of M221/mL (24 h point time) at 25 °C. At 28 h culture at 25 °C, the P450 level decreased. The MG1655 strain showed the capability of producing the highest expression level of M221 among tested strains (Figure 4B).

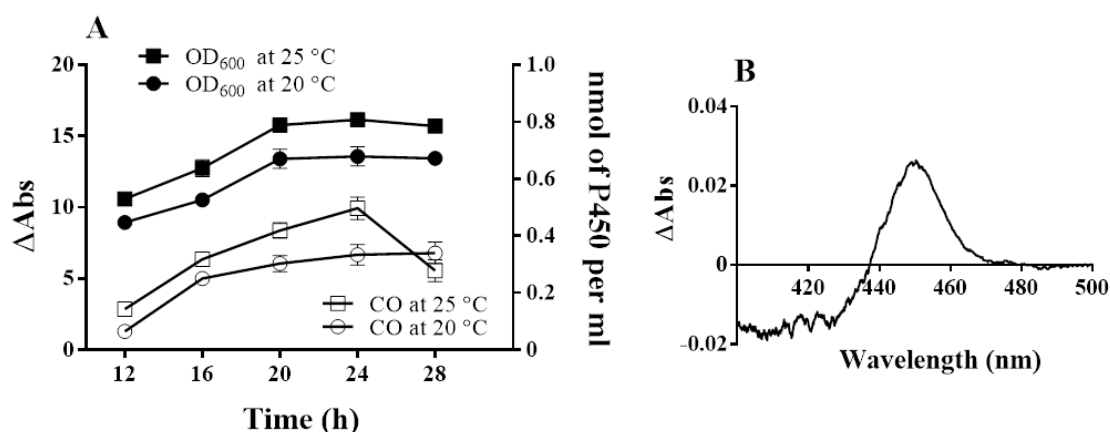


**Figure 4.** Optimal expression of CYP102A1 M221 mutant in the *E. coli* strain MG1655. (A) The cultures were grown at 20 or 25 °C up to 28 h. OD<sub>600</sub> and P450 concentration were measured at indicated time. (B) CO-difference spectrum of M221 at 24 h culture time at 25 °C.

## 2.3. Characterizing a Major Product of Naringin DC by CYP102A1 Mutants

Products and the substrate were characterized by results of the HPLC (Figure 3), LC-MS (Figures 5 and 6), and NMR spectroscopy (Figure 7). Naringin DC's minor and major products made by CYP102A1 mutants were M1 and neoeriocitrin DC, respectively. The formation of a monohydroxylated product as a major product was confirmed by LC-MS (Figure 5). The minor product (M1) has  $m/z$  596, which indicates two protons were deleted from the monohydroxylated product ( $m/z$  598). However, the M1 product formation rate is too low ( $1.5 \text{ min}^{-1}$ ) compared to that of the major product ( $8.4 \text{ min}^{-1}$ ) (Figure 3). Here, we mainly focus on the production of the major catechol product.

The major product was prepared by preparative HPLC (Figure 6), and its chemical structure was identified by NMR (Figure 7). The chemical shifts and splitting patterns of the major product's <sup>1</sup>H and <sup>13</sup>C NMR spectra are shown (see also Supplementary Figure S1–S3 for NMR spectra).

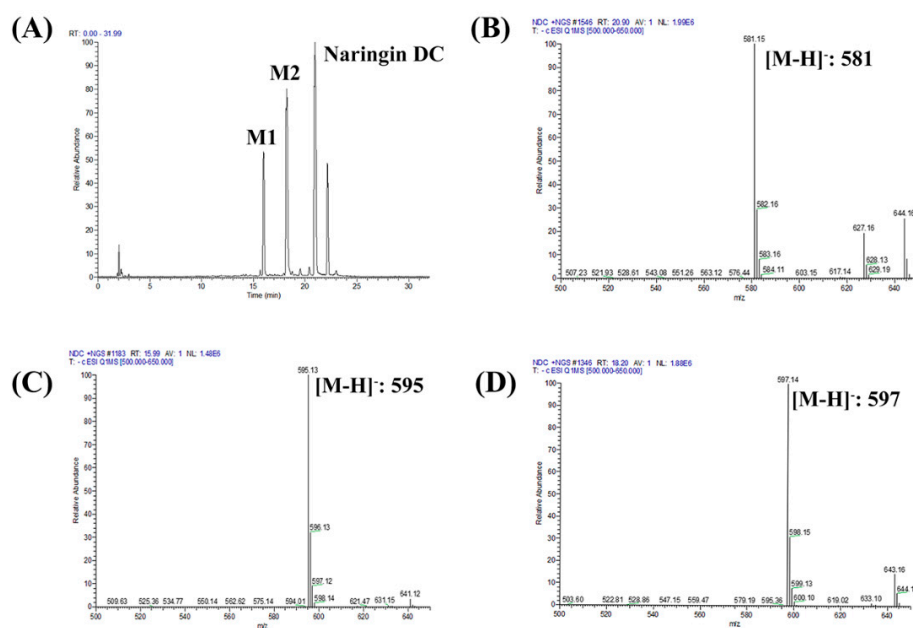


**Figure 5.** LC-MS analysis of naringin DC and its products produced by CYP102A1 M221 mutant. (A) LC-MS chromatogram of naringin DC and its products; (B) Naringin DC shows  $m/z$  582; (C) The minor product (M1) shows  $m/z$  596; (D) The major product (M2) of  $m/z$  598 was found to be monohydroxylated.

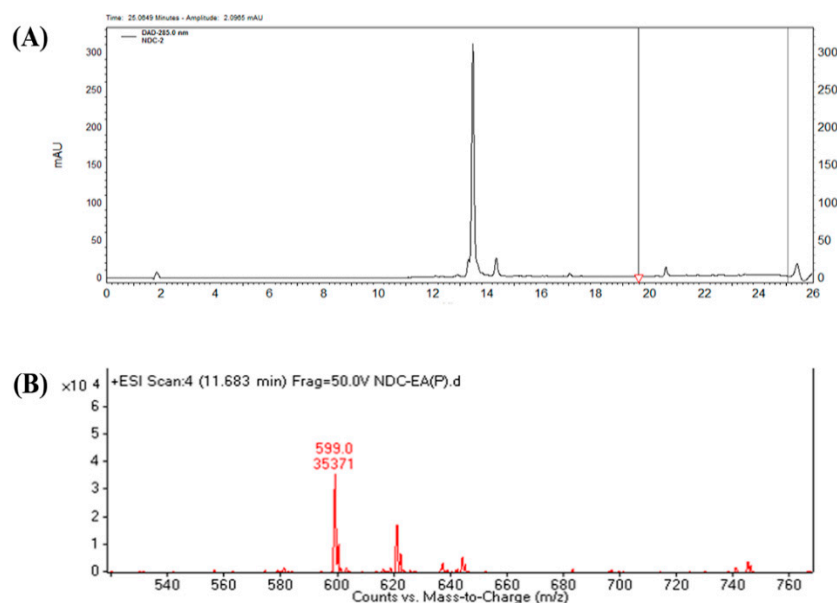


**Figure 6.** HPLC and LC-MS analyses of naringin DC's major product produced by CYP102A1 M221 mutant. (A) preparative-HPLC chromatogram of the major product of naringin DC (C18 column, 10 × 150 mm, gradient from 10% to 100% methanol, 3 mL/min). (B) LC-MS analyses of the major product DC  $[M+H]^+$  599 ( $m/z$  598).

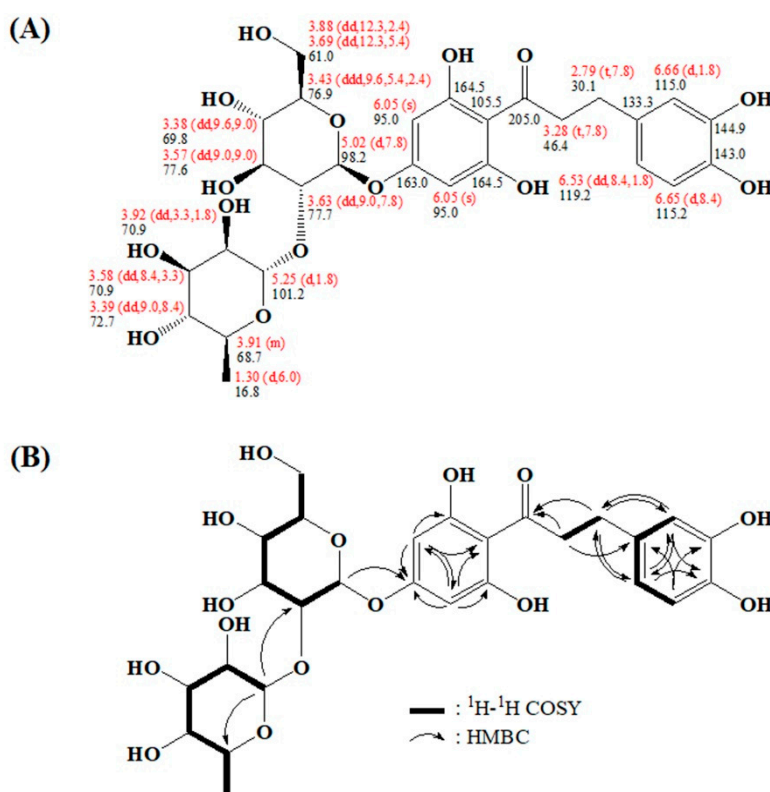


**Figure 7.** (A) Chemical structure of the major product (neoeriocitrin DC) from naringin DC. Red: <sup>1</sup>H chemical shift values (multiplicity and coupling constants [Hz] in parenthesis); Black: <sup>13</sup>C chemical shift values which were assigned from 2D HMBC NMR spectra. (B) 2D NMR spectra of the major product, neoeriocitrin DC. (See also Supplementary Figure S1–S3 for NMR spectra.)

#### 2.4. Kinetic Parameters and TTNs of Naringin DC Hydroxylation by CYP102A1 Mutants

Six mutants (M16V2, G1, M179, M221, M620, and M850) that showed high rates of naringin DC product formation among tested mutants were selected and used to measure the kinetic parameters of naringin DC hydroxylation (Table 1). WT CYP102A1 did not exhibit appreciable activity by which to determine reliable kinetic parameters. M16V2 was used as a control because it was used as a template for the DNA library. The  $k_{cat}$  values of mutants G1 (11 min<sup>-1</sup>) and M221 (10.8 min<sup>-1</sup>) increased compared to M16V2 by 41% and 38%, respectively. The  $K_m$  values of G1, M179, and M221 decreased to half, and mutants M620 and M850 showed 1.5–2.8-fold increases in  $K_m$  values when compared to that of M16V2. The catalytic efficiencies ( $k_{cat}/K_m$ ) of neoeriocitrin DC formation by mutants G1, M179, and M221 were 0.151, 0.070, and 0.137 (min<sup>-1</sup>μM<sup>-1</sup>), which were more efficient than that of M16V2 by 3.1-, 1.4-, and 2.8-fold, respectively. M620 and M850 showed decreased catalytic efficiencies due to increased  $K_m$  values.

**Table 1.** Kinetic parameters of naringin DC hydroxylation by CYP102A1. The chimeric mutant M16V2 and selected mutants (G1, M179, M221, M620, and M850).

Enzymes	$k_{cat}$ (min <sup>-1</sup> )	$K_m$ (μM)	$k_{cat}/K_m$ (min <sup>-1</sup> μM <sup>-1</sup> )
M16V2	7.8 ± 0.5	160 ± 25	0.049 ± 0.008
G1	11.0 ± 0.3	73 ± 5	0.151 ± 0.011
M179	5.3 ± 0.2	76 ± 9	0.070 ± 0.008
M221	10.8 ± 0.2	79 ± 6	0.137 ± 0.011
M620	5.7 ± 0.7	441 ± 101	0.013 ± 0.003
M850	4.5 ± 0.4	243 ± 43	0.019 ± 0.004

Four mutants (M16V2, G1, M221, and M850) were selected and used to measure the TTNs of naringin DC hydroxylation. When the assays were carried out at the reaction times of 20 min, 30 min, 1 h, 2 h, and 4 h, overall product formation was in the range of 105 to 315 TTNs (Figure 8). All mutants showed increased neoeriocitrin DC formation rate, which was 1.1–1.8-fold higher than M16V2 during indicated reaction time. In addition, the results showed that neoeriocitrin DC is stable at least up to 2 h and then the product seems to degrade. For a 1 h reaction with M221 or G1, the productivity was  $1.1 \text{ mM h}^{-1}$ , which corresponds to  $0.65 \text{ g L}^{-1} \text{ h}^{-1}$ .

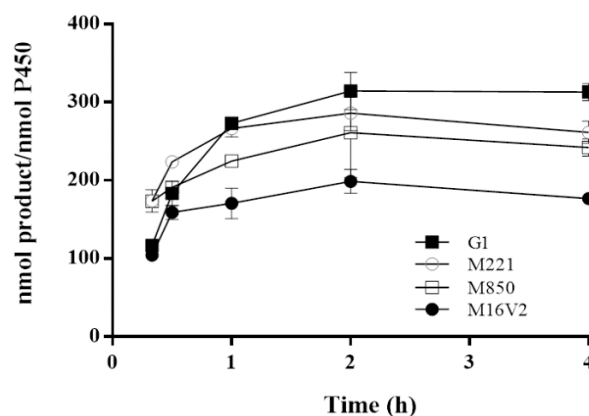


**Figure 8.** TTNs of naringin DC hydroxylation by CYP102A1 mutants. The reactions contained  $500 \mu\text{M}$  naringin DC substrate and  $0.40 \mu\text{M}$  of M16V2, G1, M221, or M850 in a 100-mM potassium phosphate buffer (pH 7.4). NADPH-generating systems were added to initiate the reaction, and the reaction mixtures were incubated for 20 min, 30 min, 1 h, 2 h, and 4 h at  $37 \text{ }^\circ\text{C}$ .

### 2.5. Spectral Titration of Naringin DC toward CYP102A1 Mutants

The differences of binding affinity between M16V2 and selected mutants toward the substrate naringin DC were analyzed by spectral binding titration (Figure 9). Binding of naringin DC to CYP102A1 G1, M179, and M221 produced a typical Type II spectral shift, with an increase at 420 nm and a decrease at 390 nm, indicating an increase in the low-spin fraction of the enzyme. The spectrally determined dissociation constants ( $K_d$ ) of naringin DC to G1, M179, and M221 were 1.6, 2.2, and  $1.4 \mu\text{M}$ , respectively (Figure 9). This result indicates that naringin DC can bind to the active sites of the mutants with a high affinity ( $K_d$  of 1–2  $\mu\text{M}$ ). However, M16V2 did not show an apparent spectral change.

It was suggested that the catechol moieties of polyphenol compounds are important for their biological antiadipogenesis, antiobesity, and anticancer functions [27]. The biological activities of resveratrol and its catechol product, piceatannol, were reported to have antioxidation, antiobesity, anti-inflammatory and anticancer abilities [28–30]. Piceatannol was shown to be more potent than resveratrol in inhibitory effects on adipogenesis, obesity, and carcinogenesis [31]. Polydatin, a glycoside of resveratrol, was reported to have many biomedical properties related to antioxidation, antiplatelet aggregation, cardioprotective activity, and anti-inflammatory and immune-regulating functions [32]. Astringin, a catechol product of polydatin, was found to have a more potential antioxidative activity than polydatin [33] and a potential cancer chemopreventive activity [34]. Moreover, 7,3'4'-trihydroxyisoflavone (7,3'4'-THIF) (a catechol product of daidzein), but not daidzein itself, inhibited UVB-induced skin tumor in hairless mice. Thus, 7,3'4'-THIF is considered a new candidate chemoprotective agent [35]. Recently, we found that 3-OH phloretin, a catechol product of phloretin, shows an inhibitory effect on adipocyte differentiation [36]. All of the catechol products mentioned above can be efficiently produced using bacterial P450s [19,22,36,37].

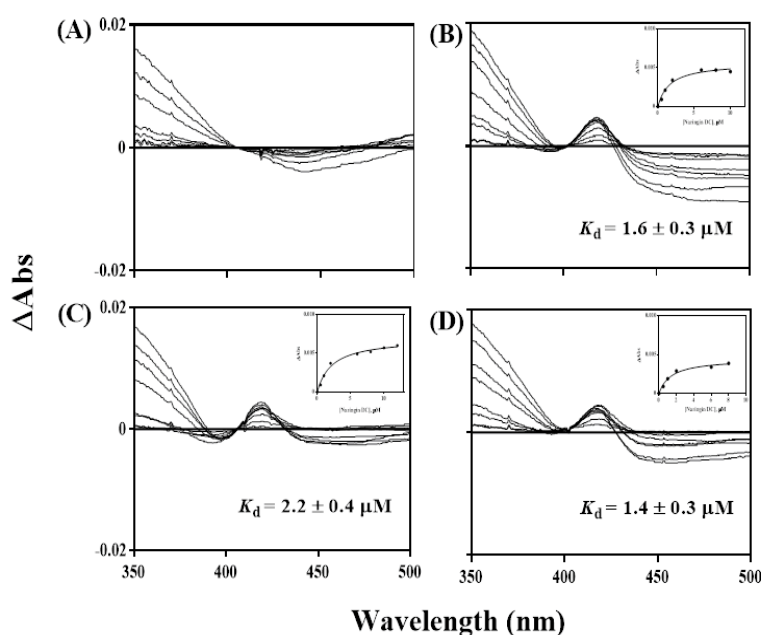


**Figure 9.** Binding titration of naringin DC to CYP102A1. The assay contained 0–20  $\mu\text{M}$  naringin DC substrate in 100 mM potassium phosphate buffer (7.4) and 1.0  $\mu\text{M}$  of M16V2 (A), G1 (B), M179 (C), and M221 (D). The inset of each panel (B–D) shows a plot of induced Soret absorbance change ( $\Delta A_{390-420}$ ) versus the relevant concentration of naringin DC. Spectrally determined dissociation constants ( $K_d$ ) were also shown.

It is known that glycosylation is an essential mechanism for diverse biological functions and the structure of natural flavonoids in plants [38,39]. Glycosylation of flavonoids can modify color and taste properties [39,40]. Furthermore, it leads to their strong solubility and stability in water [41–43], which helps to improve physiological and pharmacological properties that increase compound bioavailability [43,44]. Naringin DC is a glycoside of phloretin that shows several beneficial antioxidant, anticancer [45,46], and antiobesity [47] effects. Phloretin is widely used as a cosmeceutical ingredient for UV protection [48]. However, the biological functions of a catechol product of naringin DC, neoeriocitrin DC, have not been reported until now. Therefore, the production of neoeriocitrin DC from naringin DC by CYP102A1 reported here should be a good strategy to obtain it. Furthermore, toxicological research is needed if neoeriocitrin DC is applied as a sweetener.

In this study, we found that neoeriocitrin DC, can be produced by an enzymatic biotransformation using CYP102A1. It is now possible to study neoeriocitrin DC's biological functions, such as its antiobesity, anti-inflammatory, and anticancer abilities. Further investigation is necessary to improve the production of neoeriocitrin DC to meet the minimum space-time yield and a minimum final product concentration for industrial application [49]. Although we tried whole-cell biocatalysis experiments with *E. coli* expressing CYP102A1 genes for improved production of neoeriocitrin DC, no products of naringin DC were obtained (results not shown). Surface display [50] and export of CYP102A1 to the periplasmic space [51] of *E. coli* might be good whole cell systems for the industrial application. This result indicates that the carbohydrate moiety of naringin DC, may inhibit its transport into the *E. coli* cells because phloretin, the aglycone of naringin DC, can enter into the cells and be hydroxylated to 3-OH product [36].

### 3. Materials and Methods

#### 3.1. Materials

Glucose-6-phosphate, glucose-6-phosphate dehydrogenase from baker's yeast, naringin DC, and  $\beta$ -nicotinamide adenine dinucleotide phosphate (NADP<sup>+</sup>) were purchased from Sigma-Aldrich (St. Louis, MO, USA). Other chemicals and solvents with the highest grade were obtained from commercial suppliers

#### 3.2. Optimal Expression of CYP102A1 M221 Mutant

The plasmid of M221 (in pCW vector) was transformed to a set of competent *E. coli* cells (DH5 $\alpha$ -F'IQ, BL21, SHuffle T7, Rosetta, MG1655, and JM109) and spread on Luria-Bertani agar plate with ampicillin (100  $\mu$ g/mL). The single colony was grown in 5 mL of Luria-Bertani medium supplemented with ampicillin (100  $\mu$ g/mL) with shaking at 170 rpm overnight while maintaining 37 °C. The aliquots of cell culture (1% *v/v*) were inoculated in 50 mL of Terrific Broth medium supplemented with ampicillin (100  $\mu$ g/mL). The cells were grown at 37 °C with shaking at 170 rpm to an OD<sub>600</sub> of approximately 0.6–0.8. Then, isopropyl- $\beta$ -D-thiogalactopyranoside (0.5 mM) and  $\delta$ -aminolevulinic acid (1.0 mM) were added for enzyme expression. After the cultures were allowed to grow at 20 or 25 °C with 150 rpm, OD<sub>600</sub> and CO spectra were measured at culture times of 12, 16, 20, 24, and 28 h. CYP102A1 (P450) concentrations of whole cells were determined from the CO-difference spectra using an extinction molecular coefficient,  $\epsilon = 91$  mM/cm [26].

#### 3.3. CYP102A1 Mutants Used to Screen Highly Active Naringin DC Hydroxylases

An extensive set of CYP102A1 mutants was generated in previous work [12,14,19,22–25], and the WT BM3 and 60 mutants were used for screening highly active mutants towards naringin DC.

To make more active mutants having naringin DC hydroxylase activity, a random mutagenesis was performed to make a DNA library of the M16V2 heme domain. The chimeric protein M16V2 was originally made by exchanging the reductase domain of M16 with that of CYP102A1 natural variant V2, as described [21,24]. The error-prone PCR was performed on the CYP102A1 heme domain (1st–430th amino acid residues) of the M16V2 to make a DNA library. Oligonucleotide primers were used to introduce the BamHI/SacI restriction sites: BamHI forward, 5'-ataGGATCCatgacaattaagaaatg cctc-3' and SacI reverse, 5'-ataGAGCTCgtagtttgatgatcttcaaagctaaag tg-3'. DNA libraries of random mutants were constructed using a reaction mixture (50  $\mu$ L) of 10 pmol of each primer, 0.2 mM dNTP (0.05 mM each of dATP, dGTP, dCTP, and dTTP), Taq DNA polymerase (5 units/ $\mu$ L), MgCl<sub>2</sub> (2.5 or 5 mM), and MnCl<sub>2</sub> (0.1 or 0.15 mM) in 10 mM Tris-HCl containing 50 mM KCl (pH 8.4, 25 °C).

The PCR reaction was started at 95 °C for 5 min and run through 26 thermocycles of 95 °C for 60 s, 58 °C for 60 s, and 72 °C for 90 s. After completing the reaction, the reaction medium was held at 72 °C for 5 min and subsequently soaked at 4 °C. The amplified PCR library fragments were purified and cloned into the pCWBM3M16V2/BamHI/SacI vector using the restriction sites of BamHI and SacI. The mutation rate (2.9 mutations per 1290 bp) was validated by sequencing 12 randomly selected clones before screening of expression level and activity. The size of the screened mutant library was approximately  $1.0 \times 10^6$ .

Seven mutants selected based on a blue colony-based colorimetric method and hydroxylation activity toward naringin DC were expressed in the *E. coli* strain DH5 $\alpha$ F'-IQ. The CYP102A1 is expressed in cytosol and partially purified as supernatant lysate after removal of cell debris and membrane fractions [24]. The lysate was used to determine the CYP102A1 (P450) concentrations from the CO-difference spectra [26]. For the M16V2 and its mutants, a typical culture yielded 300 to 700 nM of P450.

### 3.4. Hydroxylation of Naringin Dihydrochalcone by CYP102A1 Mutants

The reaction mixtures contained 200  $\mu\text{M}$  naringin DC substrate in 100 mM potassium phosphate buffer (pH 7.4) and 0.20  $\mu\text{M}$  CYP102A1. An aliquot of a NADPH-generating system (10 mM glucose-6-phosphate, 0.5 mM  $\text{NADP}^+$ , and 1.0 UI yeast glucose-6-dehydrogenase/mL) was added to the initial reaction. The reaction mixture was incubated for 30 min at 37 °C and stopped by 600 mL ice-cold ethyl acetate.

The naringin DC and its products were analyzed by HPLC using a Gemini C18 column (4.6  $\times$  150 mm, 5  $\mu\text{m}$ , 110 Å; Phenomenex, Torrance, CA, USA) with the mobile phase A (water containing 0.5% methanol and 0.1% formic acid) and the mobile phase B (acetonitrile) [52]. The flow rate of the elution column was 1.0 mL/min by a gradient pump (LC-20AD; Shimadzu, Kyoto, Japan) with the following gradient: 0–3 min controlled at 9% mobile phase B, 3–20 min gradually increased reaching to 30% mobile phase B, 20–21 min decreased to 9% mobile phase B, and 21–30 min controlled at 9% mobile phase B and detected by UV at 285 nm.

The kinetic parameters of CYP102A1 mutants were determined by reaction, including 10–500  $\mu\text{M}$  of naringin DC in 100 mM potassium phosphate buffer (pH 7.4) and 0.20  $\mu\text{M}$  enzymes. The NADPH-generating systems were added to the initial reaction and the reaction mixtures were incubated for 30 min at 37 °C. A stock of substrate solution was prepared in methanol and diluted in the enzymatic reactions to the final organic solvent concentration of <1% (*v/v*). The kinetic parameter results were analyzed using GraphPad Prism software (Graph, San Diego, CA, USA).

The TTNs of CYP102A1 mutants were determined by reaction contained in 500  $\mu\text{M}$  naringin DC in 100 mM potassium phosphate buffer (pH 7.4) and 0.40  $\mu\text{M}$  enzymes. The NADPH-generating systems were added to the initial reaction and the reaction mixtures were incubated for 20 min, 30 min, 1 h, 2 h, and 4 h at 37 °C.

### 3.5. LC-MS Analysis

To identify the minor and major products of naringin DC produced by CYP102A1 mutants, a liquid chromatography–mass spectrometry (LC–MS) analysis was performed, and the LC profile and fragmentation patterns of the authentic compounds (naringin DC and neoeriocitrin DC) were compared on a Thermo Scientific Accela™ and TSQ Quantum™ Access MAX system with the heated electrospray ionization interface with HESI II probe (Thermo Fisher Scientific, Waltham, MA, USA) (Figure 5). The oxidation reaction of naringin DC by CYP102A1 was performed as described above. The separation was performed on a Zorbax SB-C18 (4.6  $\times$  250 mm, 5  $\mu\text{m}$ , 80 Å; Agilent Technologies, Santa Clara, CA, USA); the gradient mobile phase was 0.5% (*v/v*) methanol and 0.1% formic acid (*v/v*) in water (A) in acetonitrile (B), delivered at a flow rate of 1.0 mL/min. The initial composition of mobile phase B was 9%; after 3 min the mobile phase B composition increased to 30% over 17 min, decreased to 9% over 2 min, and finally re-equilibrated to the initial conditions over 13 min. Thus, the total run time was 35 min. The temperatures of the column and autosampler were kept at 40 and 4 °C, respectively, and the injection volumes were 5  $\mu\text{L}$  for all samples tested here. The electrospray ionization procedure was performed in the negative ion mode. The spray voltage was 3500 V and vaporizer temperature was 300 °C. Capillary temperature was 200 °C. Nitrogen sheath gas and auxiliary gas pressures were 40 psi and 12 psi, respectively. All data were acquired with full scan mass spectrometry (full scan) or single ion monitoring (SIM) in the negative ion detection mode using Xcalibur™ 3.0 software.

To confirm the purity of the naringin DC product produced by the CYP102A1 mutants and purified by preparative HPLC, an LC–MS analysis of products was performed to compare LC profiles and fragmentation patterns with those of the authentic compounds (naringin DC and neoeriocitrin DC) (Figure 6). The mutant M221 was included with 200  $\mu\text{M}$  naringin DC for 50 min at 37 °C with the NADPH-generating system and performed using Applied Biosystems' QTRAP-3200 mass spectrometer (Waltham, MA, USA) having LC-MS solution software.

### 3.6. NMR Spectroscopy

After the major product of naringin DC was produced by the M221, separated by preparative HPLC (C18 column, 10 × 150 mm, gradient from 10% to 100% methanol, 3 mL/min), and collected in an ice bucket, the solvent was then removed by freezer-dryer. NMR investigations were performed at ambient temperature on a JNM-ECA600 600MHz FT-NMR spectrometer (JEOL Ltd., Tokyo, Japan). CD<sub>3</sub>OD was used as solvent, and chemical shifts for proton NMR spectra were measured in parts per million (ppm) relative to tetramethylsilane.

### 3.7. Spectral Binding Titration

Spectral determinations of  $K_d$  values for the binding of substrates to the P450s were performed as described [53]. The binding affinity of naringin DC to four CYP102A1 mutants was determined (at 23 °C) by titrating 1.0 μM enzyme in 100 mM potassium phosphate buffer (pH 7.4). The absorption difference between 350 and 500 nm was plotted against the substrate concentration (0–20 μM). The  $K_d$  values were estimated using GraphPad Prism software (GraphPad Software, San Diego, CA, USA).

## 4. Conclusions

An enzymatic strategy for the efficient synthesis of a potentially valuable product from naringin DC, a glycoside of phloretin, was developed using *Bacillus megaterium* CYP102A1 monooxygenase. At present, no enzymatic or chemical methods to make products of naringin DC by hydroxylation reactions have not been reported. In this study, a set of CYP102A1 mutants was used to catalyze the hydroxylation of naringin DC. We found that the major product is neoeriocitrin DC by NMR and LC-MS analyses. Sixty seven mutants of CYP102A1 were tested for hydroxylation of naringin DC to produce neoeriocitrin DC. Six mutants with high activity were selected to determine the kinetic parameters and total turnover numbers (TTNs). The  $k_{cat}$  value of the most active mutant was 11 min<sup>-1</sup> and its TTN was 315. The productivity of neoeriocitrin DC production increased up to 1.1 mM h<sup>-1</sup>, which corresponds to 0.65 g L<sup>-1</sup> h<sup>-1</sup>. We achieved an efficient regioselective hydroxylation of naringin DC to produce neoeriocitrin DC, a catechol product.

**Supplementary Materials:** The following are available online at <http://www.mdpi.com/2073-4344/10/8/823/s1>, Figure S1. <sup>1</sup>H NMR spectra of the major product, neoeriocitrin DC; Figure S2. 2D HMBC NMR spectra of the major product, neoeriocitrin DC; Figure S3. 2D COSY NMR spectra of the major product, neoeriocitrin DC; Table S1: The amino acid sequence of M16V2 and CYP102A1 mutants.

**Author Contributions:** Conceptualization, S.-J.Y., H.-S.K., and C.-H.Y.; investigation, T.H.H.N., S.-M.W., N.A.N., and G.-S.C.; writing—original draft preparation, T.H.H.N. and C.-H.Y.; supervision, S.-J.Y., H.-S.K., and C.-H.Y.; funding acquisition, H.-S.K. and C.-H.Y. All authors have read and agreed to the published version of the manuscript.

**Funding:** This research was funded by the Next-Generation BioGreen 21 program (SSAC, grant no.: PJ01333101); Rural Development Administration and the Basic Research Lab Program (NRF-2018R1A4A1023882); National Research Foundation of Korea, Republic of Korea.

**Conflicts of Interest:** The authors declare no conflict of interest.

## References

1. Szliszka, E.; Czuba, Z.P.; Mazur, B.; Paradysz, A.; Krol, W. Chalcones and Dihydrochalcones Augment TRAIL-Mediated Apoptosis in Prostate Cancer Cells. *Molecules* **2010**, *15*, 5336–5353. [CrossRef] [PubMed]
2. Xiao, Z.; Zhang, Y.; Chen, X.; Wang, Y.; Chen, W.; Xu, Q.; Li, P.; Ma, F. Extraction, identification, and antioxidant and anticancer tests of seven dihydrochalcones from Malus “Red Splendor” fruit. *Food Chem.* **2017**, *231*, 324–331. [CrossRef] [PubMed]
3. Gaucher, M.; Dugé de Bernonville, T.; Lohou, D.; Guyot, S.; Guillemette, T.; Brisset, M.-N.; Dat, J.F. Histolocalization and physico-chemical characterization of dihydrochalcones: Insight into the role of apple major flavonoids. *Phytochemistry* **2013**, *90*, 78–89. [CrossRef] [PubMed]

4. Rozmer, Z.; Perjési, P. Naturally occurring chalcones and their biological activities. *Phytochem. Rev.* **2016**, *15*, 87–120. [[CrossRef](#)]
5. Ehrenkranz, J.R.L.; Lewis, N.G.; Kahn, C.R.; Roth, J. Phlorizin: A review. *Diabetes/Metab. Res. Rev.* **2005**, *21*, 31–38. [[CrossRef](#)]
6. Dugé de Bernonville, T.; Guyot, S.; Paulin, J.-P.; Gaucher, M.; Loufrani, L.; Henrion, D.; Derbré, S.; Guilet, D.; Richomme, P.; Dat, J.F.; et al. Dihydrochalcones: Implication in resistance to oxidative stress and bioactivities against advanced glycation end-products and vasoconstriction. *Phytochemistry* **2010**, *71*, 443–452. [[CrossRef](#)]
7. Tang, N.; Yan, W. Solubilities of Naringin Dihydrochalcone in Pure Solvents and Mixed Solvents at Different Temperatures. *J. Chem. Eng. Data* **2016**, *61*, 4085–4089. [[CrossRef](#)]
8. Yang, W.; Zhou, K.; Zhou, Y.; An, Y.; Hu, T.; Lu, J.; Huang, S.; Pei, G. Naringin Dihydrochalcone Ameliorates Cognitive Deficits and Neuropathology in APP/PS1 Transgenic Mice. *Front. Aging Neurosci.* **2018**, *10*, 169. [[CrossRef](#)]
9. Río, J.A.D.; Fuster, M.D.; Sabater, F.; Porras, I.; García-Lidón, A.; Ortuño, A. Selection of citrus varieties highly productive for the neohesperidin dihydrochalcone precursor. *Food Chem.* **1997**, *59*, 433–437. [[CrossRef](#)]
10. Nakamura, Y.; Watanabe, S.; Miyake, N.; Kohno, H.; Osawa, T. Dihydrochalcones: Evaluation as Novel Radical Scavenging Antioxidants. *J. Agric. Food Chem.* **2003**, *51*, 3309–3312. [[CrossRef](#)]
11. Liu, B.; Zhu, X.; Zeng, J.; Zhao, J. Preparation and physicochemical characterization of the supramolecular inclusion complex of naringin dihydrochalcone and hydroxypropyl- $\beta$ -cyclodextrin. *Food Res. Int.* **2013**, *54*, 691–696. [[CrossRef](#)]
12. Park, S.-H.; Kim, D.-H.; Kim, D.; Kim, D.-H.; Jung, H.-C.; Pan, J.-G.; Ahn, T.; Kim, D.; Yun, C.-H. Engineering Bacterial Cytochrome P450 (P450) BM3 into a Prototype with Human P450 Enzyme Activity Using Indigo Formation. *Drug Metab. Dispos.* **2010**, *38*, 732–739. [[CrossRef](#)] [[PubMed](#)]
13. Guengerich, F.P. Cytochrome P450 enzymes in the generation of commercial products. *Nat. Rev. Drug Discov.* **2002**, *1*, 359–366. [[CrossRef](#)] [[PubMed](#)]
14. Kim, D.-H.; Kim, K.-H.; Kim, D.-H.; Liu, K.-H.; Jung, H.-C.; Pan, J.-G.; Yun, C.-H. Generation of human metabolites of 7-ethoxycoumarin by bacterial cytochrome P450 BM3. *Drug Metab. Dispos.* **2008**, *36*, 2166–2170. [[CrossRef](#)]
15. Narhi, L.O.; Fulco, A.J. Characterization of a catalytically self-sufficient 119,000-dalton cytochrome P-450 monooxygenase induced by barbiturates in *Bacillus megaterium*. *J. Biol. Chem.* **1986**, *261*, 7160–7169.
16. Girvan, H.M.; Waltham, T.N.; Neeli, R.; Collins, H.F.; McLean, K.J.; Scrutton, N.S.; Leys, D.; Munro, A.W. Flavocytochrome P450 BM3 and the origin of CYP102 fusion species. *Biochem. Soc. Trans.* **2006**, *34*, 1173–1177. [[CrossRef](#)]
17. Urlacher, V.B.; Girhard, M. Cytochrome P450 monooxygenases: An update on perspectives for synthetic application. *Trends Biotechnol.* **2012**, *30*, 26–36. [[CrossRef](#)]
18. Whitehouse, C.J.C.; Bell, S.G.; Wong, L.-L. P450(BM3) (CYP102A1): Connecting the dots. *Chem. Soc. Rev.* **2012**, *41*, 1218–1260. [[CrossRef](#)]
19. Le, T.-K.; Jang, H.-H.; Nguyen, H.; Doan, T.; Lee, G.-Y.; Park, K.; Ahn, T.; Joung, Y.; Kang, H.-S.; Yun, C.-H. Highly regioselective hydroxylation of polydatin, a resveratrol glucoside, for one-step synthesis of astringin, a piceatannol glucoside, by P450 BM3. *Enzym. Microb. Technol.* **2016**, *97*, 34–42. [[CrossRef](#)]
20. Bernhardt, R. Cytochromes P450 as versatile biocatalysts. *J. Biotechnol.* **2006**, *124*, 128–145. [[CrossRef](#)]
21. Kang, J.-Y.; Kim, S.-Y.; Kim, D.; Kim, D.; Sun-Mi, S.; Park, S.-H.; Kim, K.-H.; Jung, H.; Pan, J.-G.; Joung, Y.; et al. Characterization of diverse natural variants of CYP102A1 found within a species of *Bacillus megaterium*. *AMB Express* **2011**, *1*, 1. [[CrossRef](#)] [[PubMed](#)]
22. Kim, D.-H.; Ahn, T.; Jung, H.-C.; Pan, J.-G.; Yun, C.-H. Generation of the human metabolite piceatannol from the anticancer-preventive agent resveratrol by bacterial cytochrome P450 BM3. *Drug Metab. Dispos.* **2009**, *37*, 932–936. [[CrossRef](#)] [[PubMed](#)]
23. Kim, K.-H.; Kang, J.-Y.; Kim, D.; Park, S.-H.; Park, S.; Kim, D.; Park, K.; Lee, Y.J.; Jung, H.; Pan, J.-G.; et al. Generation of Human Chiral Metabolites of Simvastatin and Lovastatin by Bacterial CYP102A1 Mutants. *Drug Metab. Dispos. Biol. Fate Chem.* **2010**, *39*, 140–150. [[CrossRef](#)]
24. Kang, J.-Y.; Ryu, S.H.; Park, S.-H.; Cha, G.S.; Kim, D.-H.; Kim, K.-H.; Hong, A.W.; Ahn, T.; Pan, J.-G.; Joung, Y.H.; et al. Chimeric cytochromes P450 engineered by domain swapping and random mutagenesis for producing human metabolites of drugs. *Biotechnol. Bioeng.* **2014**, *111*, 1313–1322. [[CrossRef](#)] [[PubMed](#)]

25. Jang, H.-H.; Ryu, S.-H.; Le, T.-K.; Doan, T.T.M.; Nguyen, T.H.H.; Park, K.D.; Yim, D.-E.; Kim, D.-H.; Kang, C.-K.; Ahn, T.; et al. Regioselective C-H hydroxylation of omeprazole sulfide by *Bacillus megaterium* CYP102A1 to produce a human metabolite. *Biotechnol. Lett.* **2017**, *39*, 105–112. [[CrossRef](#)] [[PubMed](#)]
26. Omura, T.; Sato, R. The carbon monoxide-binding pigment of liver microsomes. I. Evidence for its hemoprotein nature. *J. Biol. Chem.* **1964**, *239*, 2370–2378.
27. Tungmunnithum, D.; Thongboonyou, A.; Pholboon, A.; Yangsabai, A. Flavonoids and Other Phenolic Compounds from Medicinal Plants for Pharmaceutical and Medical Aspects: An Overview. *Medicines* **2018**, *5*, 93. [[CrossRef](#)]
28. Ovesná, Z.; Kozics, K.; Bader, Y.; Saiko, P.; Handler, N.; Erker, T.; Szekeres, T. Antioxidant activity of resveratrol, piceatannol and 3,3',4,4',5,5'-hexahydroxy-trans-stilbene in three leukemia cell lines. *Oncol. Rep.* **2006**, *16*, 617–624. [[CrossRef](#)]
29. Lai, T.N.H.; Herent, M.-F.; Quetin-Leclercq, J.; Nguyen, T.B.T.; Rogez, H.; Larondelle, Y.; André, C.M. Piceatannol, a potent bioactive stilbene, as major phenolic component in *Rhodomyrtus tomentosa*. *Food Chem.* **2013**, *138*, 1421–1430. [[CrossRef](#)]
30. Arai, D.; Kataoka, R.; Otsuka, S.; Kawamura, M.; Maruki-Uchida, H.; Sai, M.; Ito, T.; Nakao, Y. Piceatannol is superior to resveratrol in promoting neural stem cell differentiation into astrocytes. *Food Funct.* **2016**, *7*, 4432–4441. [[CrossRef](#)]
31. Kershaw, J.; Kim, K.-H. The Therapeutic Potential of Piceatannol, a Natural Stilbene, in Metabolic Diseases: A Review. *J. Med. Food* **2017**, *20*, 427–438. [[CrossRef](#)] [[PubMed](#)]
32. Du, Q.-H.; Peng, C.; Zhang, H. Polydatin: A review of pharmacology and pharmacokinetics. *Pharm. Biol.* **2013**, *51*, 1347–1354. [[CrossRef](#)] [[PubMed](#)]
33. Mérillon, J.-M.; Fauconneau, B.; Teguo, P.W.; Barrier, L.; Vercauteren, J.; Huguet, F. Antioxidant Activity of the Stilbene Astringin, Newly Extracted from *Vitis vinifera* Cell Cultures. *Clin. Chem.* **1997**, *43*, 1092–1093. [[CrossRef](#)]
34. Waffo-Teguo, P.; Lee, D.; Cuendet, M.; Mérillon, J.; Pezzuto, J.M.; Kinghorn, A.D. Two new stilbene dimer glucosides from grape (*Vitis vinifera*) cell cultures. *J. Nat. Prod.* **2001**, *64*, 136–138. [[CrossRef](#)]
35. Lee, D.E.; Lee, K.W.; Byun, S.; Jung, S.K.; Song, N.; Lim, S.H.; Heo, Y.-S.; Kim, J.E.; Kang, N.J.; Kim, B.Y.; et al. 7,3',4'-Trihydroxyisoflavone, a Metabolite of the Soy Isoflavone Daidzein, Suppresses Ultraviolet B-induced Skin Cancer by Targeting Cot and MKK4. *J. Biol. Chem.* **2011**, *286*, 14246–14256. [[CrossRef](#)]
36. Nguyen, N.A.; Jang, J.; Le, T.-K.; Nguyen, T.H.H.; Woo, S.-M.; Yoo, S.-K.; Lee, Y.J.; Park, K.D.; Yeom, S.-J.; Kim, G.-J.; et al. Biocatalytic Production of a Potent Inhibitor of Adipocyte Differentiation from Phloretin Using Engineered CYP102A1. *J. Agric. Food Chem.* **2020**, *68*, 6683–6691. [[CrossRef](#)]
37. Pandey, B.P.; Roh, C.; Choi, K.-Y.; Lee, N.; Kim, E.J.; Ko, S.; Kim, T.; Yun, H.; Kim, B.-G. Regioselective hydroxylation of daidzein using P450 (CYP105D7) from *Streptomyces avermitilis* MA4680. *Biotechnol. Bioeng.* **2010**, *105*, 697–704. [[PubMed](#)]
38. Thibodeaux, C.J.; Melançon, C.E.; Liu, H. Natural-product sugar biosynthesis and enzymatic glycodiversification. *Angew. Chem. Int. Ed. Engl.* **2008**, *47*, 9814–9859. [[CrossRef](#)]
39. Gutmann, A.; Bungaruang, L.; Weber, H.; Leybold, M.; Breinbauer, R.; Nidetzky, B. Towards the synthesis of glycosylated dihydrochalcone natural products using glycosyltransferase-catalysed cascade reactions. *Green Chem.* **2014**, *16*, 4417–4425. [[CrossRef](#)]
40. Bowles, D.; Isayenkova, J.; Lim, E.-K.; Poppenberger, B. Glycosyltransferases: Managers of small molecules. *Curr. Opin. Plant Biol.* **2005**, *8*, 254–263. [[CrossRef](#)]
41. Wang, X. Structure, mechanism and engineering of plant natural product glycosyltransferases. *FEBS Lett.* **2009**, *583*, 3303–3309. [[CrossRef](#)] [[PubMed](#)]
42. Plaza, M.; Pozzo, T.; Liu, J.; Gulshan Ara, K.Z.; Turner, C.; Nordberg Karlsson, E. Substituent effects on in vitro antioxidant properties, stability, and solubility in flavonoids. *J. Agric. Food Chem.* **2014**, *62*, 3321–3333. [[CrossRef](#)] [[PubMed](#)]
43. Slámová, K.; Kapešová, J.; Valentová, K. “Sweet Flavonoids”: Glycosidase-Catalyzed Modifications. *Int. J. Mol. Sci.* **2018**, *19*, 2126. [[CrossRef](#)] [[PubMed](#)]
44. Xu, L.; Qi, T.; Xu, L.; Lu, L.; Xiao, M. Recent progress in the enzymatic glycosylation of phenolic compounds. *J. Carbohydr. Chem.* **2016**, *35*, 1–23. [[CrossRef](#)]

45. Devi, M.A.; Das, N.P. In vitro effects of natural plant polyphenols on the proliferation of normal and abnormal human lymphocytes and their secretions of interleukin-2. *Cancer Lett.* **1993**, *69*, 191–196. [[CrossRef](#)]
46. Nelson, J.A.; Falk, R.E. The efficacy of phloridzin and phloretin on tumor cell growth. *Anticancer. Res.* **1993**, *13*, 2287–2292.
47. Alsanea, S.; Gao, M.; Liu, D. Phloretin Prevents High-Fat Diet-Induced Obesity and Improves Metabolic Homeostasis. *AAPS J.* **2017**, *19*, 797–805. [[CrossRef](#)]
48. Wu, Y.; Zheng, X.; Xu, X.-G.; Li, Y.-H.; Wang, B.; Gao, X.-H.; Chen, H.-D.; Yatskayer, M.; Oresajo, C. Protective effects of a topical antioxidant complex containing vitamins C and E and ferulic acid against ultraviolet irradiation-induced photodamage in Chinese women. *J. Drugs Dermatol.* **2013**, *12*, 464–468.
49. Julsing, M.K.; Cornelissen, S.; Bühler, B.; Schmid, A. Heme-iron oxygenases: Powerful industrial biocatalysts? *Curr. Opin. Chem. Biol.* **2008**, *12*, 177–186. [[CrossRef](#)]
50. Yim, S.-K.; Kim, D.-H.; Jung, H.-C.; Pan, J.-G.; Kang, H.-S.; Ahn, T.; Yun, C.-H. Surface display of heme- and diflavin-containing cytochrome P450 BM3 in *Escherichia coli*: A whole cell biocatalyst for oxidation. *J. Microbiol. Biotechnol.* **2010**, *20*, 712–717. [[CrossRef](#)]
51. Kaderbhai, M.A.; Ugochukwu, C.C.; Kelly, S.L.; Lamb, D.C. Export of Cytochrome P450 105D1 to the Periplasmic Space of *Escherichia coli*. *Appl. Environ. Microbiol.* **2001**, *67*, 2136–2138. [[CrossRef](#)] [[PubMed](#)]
52. Remsberg, C.M.; Yáñez, J.A.; Vega-Villa, K.R.; Miranda, N.D.; Andrews, P.K.; Davies, N.M. HPLC-UV Analysis of Phloretin in Biological Fluids and Application to Pre-Clinical Pharmacokinetic Studies. *J. Chromatogr. Sep. Tech.* **2010**, *1*, 101. [[CrossRef](#)]
53. Hosea, N.A.; Miller, G.P.; Guengerich, F.P. Elucidation of Distinct Ligand Binding Sites for Cytochrome P450 3A4. *Biochemistry* **2000**, *39*, 5929–5939. [[CrossRef](#)] [[PubMed](#)]



© 2020 by the authors. Licensee MDPI, Basel, Switzerland. This article is an open access article distributed under the terms and conditions of the Creative Commons Attribution (CC BY) license (<http://creativecommons.org/licenses/by/4.0/>).